Electronic-State Dependence of Intramolecular Proton Transfer of *o*-Hydroxybenzaldehyde. 2. Substituent Effect†

Shin-ichi Nagaoka,* Yoshikazu Shinde, and Kazuo Mukai

Department of Chemistry, Faculty of Science, Ehime University, Matsuyama 790-77, Japan

Umpei Nagashima

Department of Information Sciences, Faculty of Science, Ochanomizu University, Otsuka, Bunkyo-ku, Tokyo 112, Japan

Received: September 24, 1996; In Final Form: January 21, 1997⊗

The excited-state dependence of the intramolecular proton transfer of *o*-hydroxybenzaldehyde and related molecules in the vapor phase has been studied by means of emission spectroscopy. Substituent effects on the fluorescence quantum yields from the lowest and second excited $^1(\pi,\pi^*)$ states can be explained by considering the nodal pattern of the wave function along with the delocalization of the π lone electrons in the excited state.

Introduction

For many years, much attention has been directed, from both theoretical and experimental points of view, to the excited-state intramolecular proton transfer (ESIPT) of hydrogen-bonded molecules.[1−7] ESIPT is a very simple chemical process and is readily accessible to both accurate measurements and quantitative theoretical analyses. Moreover, it plays an important role in biochemistry and practical application, and a molecule showing ESIPT can be a candidate for molecular systems such as optical memories[8] and switches.[9]

Understanding of the mechanism of ESIPT in a simple molecule can lead to valuable insights into the behavior of complex systems. *o*-Hydroxybenzaldehyde (OHBA) is the simplest and prototypical example of aromatic molecules with an intramolecular hydrogen bond involving a carbonyl group. Accordingly, we have investigated the dynamic processes in the lowest and second excited singlet states of (π,π^*) type ($S_1^{(\pi)}$ and $S_2^{(\pi)}$ states, respectively) of OHBA vapor in detail.[10−13] The main conclusions obtained previously are as follows (see Figure 1).

The stable molecular structure in the ground state (S_0 state) of OHBA is an intramolecularly hydrogen-bonded closed conformer. The potential surface of the S_0 state has only one minimum, and no S_0 state enol tautomer exists as a metastable state.

The $S_0-S_1^{(\pi)}$ absorption, fluorescence, and excitation spectra of OHBA are broad and structureless. The $S_1^{(\pi)} \rightarrow S_0$ fluorescence spectrum is highly Stokes-shifted. The emission originates not from the zwitterion but from the enol tautomer produced by ESIPT.[11,12] The potential surface of the $S_1^{(\pi)}$ state of OHBA has only one minimum and is largely distorted from that of the S_0 state owing to ESIPT.

OHBA shows fluorescence also from the $S_2^{(\pi)}$ state in the vapor phase. The $S_2^{(\pi)} \rightarrow S_0$ fluorescence quantum yield is greater than the $S_1^{(\pi)} \rightarrow S_0$ one. The $S_0-S_2^{(\pi)}$ absorption, fluorescence, and excitation spectra are structured, and the 0−0 bands are intense. The Stokes shift of the $S_2^{(\pi)} \rightarrow S_0$ fluorescence is much smaller than that of the $S_1^{(\pi)} \rightarrow S_0$ fluorescence. The potential surface of the $S_2^{(\pi)}$ state has only one minimum and is not largely distorted from that of the S_0 state. The $S_2^{(\pi)}$ state is less susceptible to ESIPT than the $S_1^{(\pi)}$ state in OHBA. The $S_1^{(\pi)} \rightarrow S_0$ fluorescence cannot be observed for excitation into the $S_2^{(\pi)}$ state.[10]

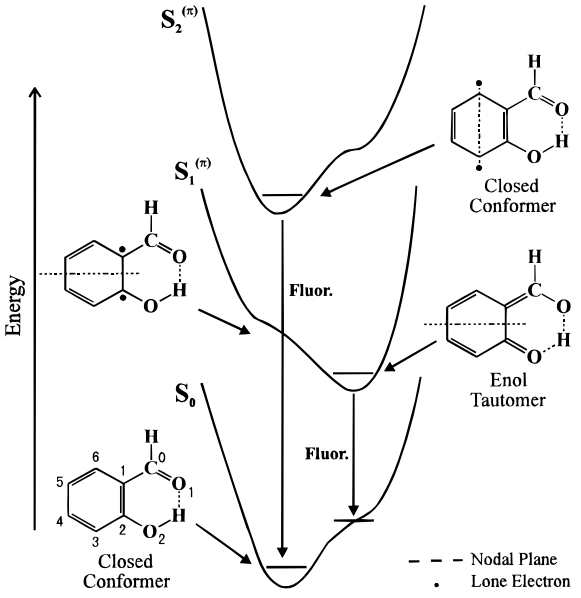

Figure 1. Schematic representation of S_0, $S_1^{(\pi)}$, and $S_2^{(\pi)}$ potential surfaces for OHBA, and numbering system for atoms used in the present work. Fluor. denotes fluorescence. For many years, the structures before and after ESIPT in OHBAs are called keto and enol forms, respectively (for example, see refs 4−6,10−13,15). Recently, the reverse was used in some papers.[16,18,20] In the present paper, we use the traditional terminology. For 2-(2-hydroxyphenyl)benzoxazole and 2-(2-hydroxyphenyl)benzothiazole, the structures before and after ESIPT are traditionally called enol and keto forms, respectively, in contrast to the cases of OHBAs (see ref 4−6).

As shown in Figure 1, the relative stability of the closed conformer and the enol tautomer of OHBA depends on the electronic state. The energy gap between the zero-point vibrational levels of the $S_1^{(\pi)}$ and $S_2^{(\pi)}$ states is large owing to ESIPT in the $S_1^{(\pi)}$ state. Under these circumstances, the $S_2^{(\pi)} \rightarrow S_1^{(\pi)}$ internal conversion must be slow, since the large energy gap reduces the Franck−Condon factor according to the energy

† This paper is dedicated to Professor Noboru Hirota of Kyoto University on the occasion of his 60th birthday. For part 1, see ref 11.

⊗ Abstract published in *Advance ACS Abstracts,* April 1, 1997.

S1089-5639(96)02948-9 CCC: $14.00

gap law. Thus, the $S_2^{(\pi)} \rightarrow S_0$ fluorescence of OHBA is observed with moderate intensity.

The reason for ESIPT of OHBA can be understood by considering the π electron nodal pattern of the wave function. In the $S_1^{(\pi)}$ state, a nodal plane passes between the two oxygen atoms and through the hydroxyphenyl ring as shown in Figure 1. The nodal plane runs perpendicular to the molecular plane. Then, one can write two double bonds along the nodal plane, because π electrons are distributed over the molecule except on the nodal plane. When the two double bonds are $C_3{=}C_4$ and $C_5{=}C_6$, apparent π lone electrons are localized at C_1 and C_2 atoms. The lone electrons facilitate the rearrangement of bonds to produce the enol tautomer. This rearrangement and the delocalization of the lone electrons significantly lower the energy of the excited state. Thus, the enol tautomer is preferred owing to the favorable nodal pattern in the $S_1^{(\pi)}$ state of OHBA. This explanation is consistent with the results of ab initio calculations on ESIPT of OHBA.[12]

In contrast, the wave function in the $S_2^{(\pi)}$ state of OHBA shows a nodal plane perpendicular to that in the $S_1^{(\pi)}$ state (Figure 1). ESIPT to yield the enol tautomer cannot take place in the $S_2^{(\pi)}$ state, because $C_0{=}C_1$ and $C_2{=}O_2$ bonds cannot be formed. As a result, the potential surface of the $S_2^{(\pi)}$ state is not largely distorted from that of the S_0 state in OHBA.

In terms of our "nodal plane" model, ESIPT is described by the skeletal distortion of the aromatic ring instead of the change in the O−H···O structure. The change in electronic structure due to the $S_0 \rightarrow S_1^{(\pi)}$ excitation ($\pi \rightarrow \pi^*$ transition) mainly affects the π-bonding framework of the aromatic ring moiety instead of the σ-bonding one of the hydrogen-bonded moiety.

We reached these conclusions previously,[10−13] and many other chemists have cited our nodal plane model.[4,14−20] However, further studies are needed to clarify the dynamic processes in the $S_1^{(\pi)}$ and $S_2^{(\pi)}$ states of OHBA. First, it would be worthwhile to know whether or not $S_2^{(\pi)} \rightarrow S_0$ fluorescence of moderate intensity is generally found in similar molecules. Usually, the $S_2 \rightarrow S_0$ fluorescence quantum yield is very small compared with that of $S_1 \rightarrow S_0$. Exceptions occur only in azulenes, thiones, and other systems,[10] which exhibit strong $S_2 \rightarrow S_0$ fluorescence with very weak $S_1 \rightarrow S_0$ fluorescence. Compared with these molecules, OHBA and several carotenoids are characterized by the dual emissive state with comparative intensities from the $S_1^{(\pi)}$ and $S_2^{(\pi)}$ states.[10,11,21,22] This property is very rare in the molecules so far investigated. It seems desirable to find other examples for such an anomalous dual emission.

Secondly, it would be interesting to know how the anomalous emission property changes with respect to the substituents. Of particular interest is whether or not such a substituent effect can be explained by considering the nodal pattern of the wave function along with the delocalization of the lone electrons in the excited state.

Accordingly, in the present work, the excited-state dependence of ESIPT of OHBAs has been investigated in the vapor phase by means of emission spectroscopy. The substituent effect on ESIPT is explained in terms of the nodal pattern and the electron delocalization in the excited state.

Experimental and Computational Methods

2-(Trifluoroacetyl)phenol (TFAP) and 2-(dichloroacetyl)-phenol (DCAP) were prepared according to the methods reported previously.[23,24] OHBA, *o*-hydroxyacetophenone (OHAP), *o*-hydroxypropiophenone (OHPP), and methyl salicylate (MS) were commercially obtained. The sample was purified by vacuum distillation in a grease-free vacuum line and was introduced into a quartz cell. Judging from the low vapor pressure and the short lifetimes of the $S_1^{(\pi)}$ and $S_2^{(\pi)}$ states of OHBA,[10,11] one can expect that all the optical measurements for OHBAs vapor were made under collision-free conditions.

We also tried to obtain the fluorescence quantum yields of 2-hydroxybenzoyl chloride, 2-hydroxybenzoyl cyanide, salicylamide, and 2-(trichloroacetyl)phenol. However, these molecules are difficult to be synthesized, are unstable, or have too low vapor pressures to estimate the reliable values of the quantum yields. Further details of these molecules are available as Supporting Information.

The fluorescence quantum yields at room temperature were determined as described below. The absorption spectra were taken with a Shimadzu UV-2100S spectrophotometer. The fluorescence spectra were measured with a Shimadzu RF-5000 spectrofluorophotometer or an emission spectrophotometer designed in our laboratory. The spectrophotometer is based on the photon-counting method and consists of a 150 W xenon arc lamp, an excitation grating monochromator of a Shimadzu RF-5000 spectrofluorophotometer, a Nikon G-250 emission grating monochromator, and a Hamamatsu R585 photomultiplier detector. The fluorescence spectral signals were transferred to an NEC PC9801DX/U2 microcomputer and analyzed using the method of Mimuro et al.[25] The fluorescence quantum yields were determined by comparing the fluorescence spectra of the sample vapor with that of quinine sulfate in 1 N sulfuric acid,[26] after the fluorescence spectra concerned had been corrected for the spectral sensitivity of the detector. The actual absorption and fluorescence spectra of OHBAs were given in the Supporting Information section.

The computational method and procedure were also given in the Supporting Information section, together with the optimized geometries of OHBAs.

TABLE 1: ϕ_1 and ϕ_2 of OHBAs and Yukawa-Tsuno's σ_π Constants of Substituents Bonded to Carbonyl Carbon

	ϕ_1[a]	ϕ_2[a]	σ_π
OHBA	5.3×10^{-5}	1.6×10^{-4}	0
TFAP	1.6×10^{-5}	3.3×10^{-4}	0.24
OHAP	4.3×10^{-4}	6.2×10^{-5}	−0.078
OHPP	2.2×10^{-5}	5.9×10^{-6}	−0.069
MS	4.4×10^{-4} [b]	4.5×10^{-5}	−0.281

[a] The same quantum yields within the experimental errors (±10%) were obtained at least twice. [b] MS shows dual $S_1^{(\pi)} \rightarrow S_0$ fluorescence, one in UV and the other in the visible region, originating from the closed conformer and its rotamer of the S_0 molecules (ref 15 and references cited therein). We need ϕ_1 of the closed conformer (fluorescence quantum yield in the visible region) in the present study. The value of the absorbance used in the estimation of ϕ_1 is larger than the real one of the closed conformer, because the observed one is made up by the superposition of those of the two conformers. Thus, the real ϕ_1 for the closed conformer of MS is considered to be larger than that given here. OHBA, TFAP, OHAP, and OHPP show the $S_1^{(\pi)} \rightarrow S_0$ fluorescence emission in the visible region alone, which originates from the closed conformers.

Results and Discussion

In the vapor phase, TFAP, DCAP, OHAP, OHPP, and MS show $S_2^{(\pi)} \rightarrow S_0$ fluorescence emissions in addition to the $S_1^{(\pi)} \rightarrow S_0$ ones, as well as OHBA; the $S_1^{(\pi)} \rightarrow S_0$ and $S_2^{(\pi)} \rightarrow S_0$ emissions are located in the wavelength ranges 400−650 and 250−350 nm, respectively. The $S_2^{(\pi)} \rightarrow S_0$ fluorescence emissions of OHBAs provide other examples of anomalous dual emissions.

The $S_1^{(\pi)} \rightarrow S_0$ and $S_2^{(\pi)} \rightarrow S_0$ fluorescence quantum yields (ϕ_1 and ϕ_2, respectively) of OHBA, TFAP, OHAP, OHPP, and MS are given in Table 1, together with Yukawa−Tsuno's σ_π

constants[27] of the substituents bonded to the carbonyl carbon. σ_π is a type of Hammett's parameter. Yukawa and Tsuno expressed a parameter corresponding to σ in the Hammett equation by $\sigma_i + r\sigma_\pi$, where σ_i is a normal substituent constant which does not involve any additional π-electronic interaction between the substituent and the reaction center. The σ_π is the resonance substituent constant measuring the capability for π-delocalization of the π-electron donor or π-electron acceptor substituent. The r value is a parameter characteristic for the given reaction, measuring the extent of resonance demand. The σ_π value does not depend on the substituted position. The reference system used in the development of these parameters is the same as the Hammett equation. Yukawa−Tsuno's constants are applicable to various substituted positions of many molecules other than benzene derivatives.[27]

The values of ϕ_1 and ϕ_2 of OHPP are very small compared with most of ϕ_1 and ϕ_2 of the other molecules, respectively (Table 1). The reason for this might be ascribed to the fact that the density of vibrational states of OHPP is significantly higher owing to the CH_2CH_3 group. Except for OHPP, ϕ_1 and ϕ_2 decreases and increases with increasing σ_π, respectively. In DCAP, ϕ_1 is less than ϕ_2, but the vapor pressure is too low to estimate the reliable values of ϕ_1 and ϕ_2.

In the decay from the $S_1^{(\pi)}$ and $S_2^{(\pi)}$ states, the nonradiative decay rate is much larger than the radiative one (Table 1). The $S_2^{(\pi)} \rightarrow S_1^{(\pi)}$ internal conversion is considered to be dominant in the nonradiative decay from the $S_2^{(\pi)}$ state.[10−13] Candidates for the nonradiative decay process from the $S_1^{(\pi)}$ state are $S_1^{(\pi)} \rightarrow S_0$ internal conversion and/or intersystem crossing to a triplet state. The $S_1^{(\pi)} \rightarrow S_0$ decay rate constant in solutions can be analyzed in terms of the sum of the temperature-independent and -dependent decay rate constants;[28−31] the intersystem crossing and the radiative processes in the enol tautomer are temperature independent, and the temperature-dependent decay process, which is dominant at room temperature, is identified as the $S_1^{(\pi)} \rightarrow S_0$ internal conversion.[31] Accordingly, it seems likely that the $S_1^{(\pi)} \rightarrow S_0$ internal conversion is dominant in the nonradiative decay from the $S_1^{(\pi)}$ state under present experimental conditions.

When a large energy gap induces slow $S_2^{(\pi)} \rightarrow S_1^{(\pi)}$ internal conversion as in OHBAs, it is fruitful to examine the value of the logarithm of the relative fluorescence quantum yield (log ϕ_1/ϕ_2) as reported previously;[21,22] log ϕ_1/ϕ_2 is related to the energy gaps between the S_0 and $S_1^{(\pi)}$ states and between $S_1^{(\pi)}$ and $S_2^{(\pi)}$ states, according to the energy gap law.[32] Hammett's rule is also applicable to spectroscopic data such as the shifts of energy levels;[27] as described below, only the $S_1^{(\pi)}$ state is shifted owing to the substituent effect in the simple picture of the present case. Plots of experimental data vs σ_π are useful in the present case in which π-electron interaction plays a major part as described below. We have thus plotted log ϕ_1/ϕ_2 of OHBAs against the σ_π values (Figure 2). The plot indicates a linear relationship with a negative slope. As the electron-withdrawing property of the substituent bonded to the carbonyl carbon increases, ϕ_1/ϕ_2 decreases.

The reason for this substituent effect can be explained by considering the nodal pattern of the wave function and the delocalization of the lone electrons in the excited state (Figure 3). In TFAP, owing to the electron-withdrawing substituent, the π lone electron on C_1 is significantly delocalized in the $S_1^{(\pi)}$ state (arrow in Figure 3b). Owing to the delocalization of the lone electron on C_1 in Figure 3b, the $S_1^{(\pi)}$ state of TFAP is stabilized in comparison with that of OHBA in Figure 3a. Then, the energy gap between the zero-point vibrational levels of the $S_1^{(\pi)}$ and $S_2^{(\pi)}$ states becomes large and that between the zero-point vibrational levels of the S_0 and $S_1^{(\pi)}$ states becomes small (Figure 3b). As a result, the rates of the $S_2^{(\pi)} \rightarrow S_1^{(\pi)}$ and $S_1^{(\pi)} \rightarrow S_0$ internal conversions become slow and fast, respectively, according to the energy gap law.[32] Since the fluorescence quantum yield increases with the decrease of the internal conversion rate, ϕ_1/ϕ_2 of TFAP has to be less than that of OHBA. The situation encountered for a molecule with an electron-donating group such as OHAP (Figure 3c) is the reverse of that with an electron-withdrawing group such as TFAP (Figure 3b). The substituent effects observed here may provide important evidence that the enolic form is predominant for the $S_1^{(\pi)} \rightarrow S_0$ fluorescing species. The substituent effect on ϕ_1 of OHBAs observed in solutions[33] is also consistent with our above-mentioned explanation. The phenomena concerning ESIPT in hydroxyanthraquinones and aminoanthraquinones can similarly be explained by using the concept based on the nodal patterns.[34]

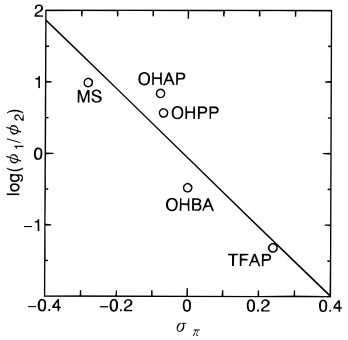

Figure 2. Plot of log ϕ_1/ϕ_2 vs σ_π of OHBAs. The plot gives a fair linear fit with a slope of -4.8, an intercept of -5.9×10^{-2}, and a correlation coefficient of 0.914.

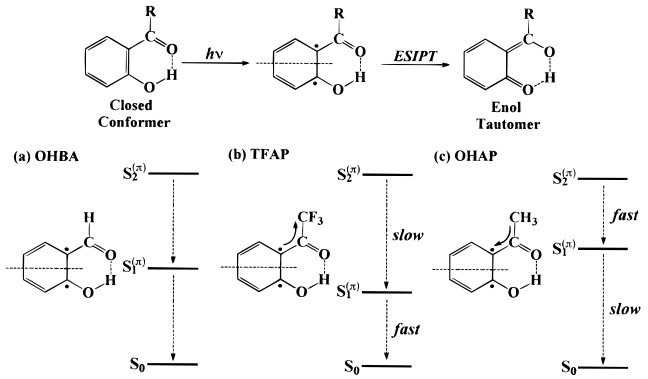

Figure 3. Schematic energy state diagram for dynamic processes in the $S_1^{(\pi)}$ and $S_2^{(\pi)}$ states of (a) OHBA, (b) TFAP, and (c) OHAP.

If the above-mentioned substituent effects based on our "nodal plane" model are absent, the fluorescence quantum yield would not show systematic dependence on the electron-donating and electron-withdrawing property of the substituent. In fact, the $S_1 \rightarrow S_0$ fluorescence quantum yields of benzene, 1,4-bis-(trifluoromethyl)benzene (CF_3-Ph-CF_3), *p*-xylene (CH_3-Ph-CH_3), and 1,4-dimethoxybenzene (CH_3O-Ph-OCH_3) in cyclohexane were estimated to be 0.07, 0.16, 0.40, and 0.21, respectively;[35] they do not show a systematic substituent effect, in contrast to ϕ_1 and ϕ_2 of OHBA, TFAP, OHAP, and MS in Table 1.

Our explanation could be strengthened if the energy of the 0−0 band of the $S_0-S_1^{(\pi)}$ transition is obtained in the vapor phase. Such an experiment requires a tunable laser and a supersonic jet apparatus,[18,36−39] which are not available to us. Accordingly, we use the energies at the $S_0-S_1^{(\pi)}$ absorption and fluorescence maxima (E_1^{a-max} and E_1^{f-max}, respectively) as measures of the energy of the 0−0 band. We have also calculated the $S_0 \rightarrow S_1^{(\pi)}$ transition energy of the closed

TABLE 2: E_1^{a-max}, E_1^{f-max}, E_1^{cal}, E_2^{a-max}, E_2^{f-max}, and E_2^{cal} of OHBAs

	E_1^{a-max} [a] (eV)	E_1^{f-max} [b] (eV)	E_1^{cal} (eV)	E_2^{a-max} [a] (eV)	E_2^{f-max} [b] (eV)	E_2^{cal} (eV)
OHBA	3.87	2.30	4.11	4.94	4.40	4.38
TFAP	3.65	2.25	3.95	4.86	4.32	4.49
OHAP	3.92	2.40	4.18	5.00	4.34	4.60
OHPP	3.81	2.43	4.21	5.02	4.68	4.69
MS	4.09	2.64[c]	4.25	5.32	4.84	4.73

[a] A typical slit width used in the measurements was 2 nm. [b] A typical fluorescence spectrum was obtained with a bandwidth of 5 nm; the excitation was made at the absorption maxima with the slit width of 15 nm. [c] Fluorescence maximum in the visible region.

conformer with the CNDO/S3 method (E_1^{cal}). Generally speaking, as the 0−0 band is red-shifted, E_1^{a-max}, E_1^{f-max}, and E_1^{cal} may decrease. It should, however, be noted that considerable vibrations are excited in the transitions at E_1^{a-max}, E_1^{f-max}, and E_1^{cal}, though the anomalous emission property of OHBAs is due to the large energy separation between the zero-point vibrational levels of the $S_1(\pi)$ and $S_2(\pi)$ states (energy gap law[32]). The values of E_1^{a-max}, E_1^{f-max}, and E_1^{cal} are listed in Table 2. As the electron-withdrawing property of the substituent bonded to the carbonyl carbon increases, E_1^{a-max}, E_1^{f-max}, and E_1^{cal} decrease. These results may also support our view. It seems that the S_0 potential surfaces of OHBAs are close in shape to one another; similar arguments hold for the $S_1(\pi)$ state, and only the $S_0-S_1(\pi)$ energy gap may change by the substituent effect.

The energies at the $S_0-S_2(\pi)$ absorption and fluorescence maxima (E_2^{a-max} and E_2^{f-max}, respectively) and the $S_0 \rightarrow S_2(\pi)$ transition energy of the closed conformer with the CNDO/S3 method (E_2^{cal}) are also listed in Table 2. In contrast to the simple scheme shown in Figure 3, the values of E_2^{a-max}, E_2^{f-max}, and E_2^{cal} are also dependent on the substituent. At present, we can offer no unambiguous explanation for this, since properties of higher-lying excited states are complex.

We have critically examined the other possibilities to explain the above-mentioned substituent effect. The electron withdrawing group bonded to the carbonyl carbon in TFAP may contribute to weakening the OH···O_1═C_0 hydrogen bond, because the substituent decreases the electron density on O_1. If this effect plays a major role in ESIPT, TFAP would be less susceptible to ESIPT than OHBA, and the stabilization of the $S_1(\pi)$ state of TFAP would be less than that of OHBA. Then, the energy gap between the zero-point vibrational levels of the $S_1(\pi)$ and $S_2(\pi)$ states of TFAP would become small, the rates of the $S_2(\pi) \rightarrow S_1(\pi)$ and $S_1(\pi) \rightarrow S_0$ internal conversions would become fast and slow, respectively, and ϕ_1/ϕ_2 of TFAP would be larger than that of OHBA. However, the experimental results are certainly the reverse of this expectation. Thus, it is considered that such an effect does not play a major role in ESIPT of OHBAs.

The fluorescence quantum yield ϕ_n ($n = 1$ and 2) is given by $\phi_n = k_n^r/(k_n^r + k_n^{nr})$, where k_n^r and k_n^{nr} are radiative and nonradiative decay rate constants, respectively. Accordingly, the substituent effects on k_1^r and k_2^r can also have an influence on ϕ_1/ϕ_2. However, k_1^r and k_2^r obtained from the absorption spectra[40] in hexane ($\approx 10^7$ and $\approx 10^8$, respectively) are almost independent of the substituent bonded to the carbonyl carbon. Accordingly, the substituent effect on ϕ_1/ϕ_2 is likely to originate not from the radiative decay but from the nonradiative decay.

In our view, susceptibility to ESIPT can be derived directly from the nature of the wave function itself; the aromatic skeleton responds to formation of a node in the $S_1(\pi)$ wave function. Our concept is simple and the idea readily provides a useful qualitative guide for predicting the more stable form in a particular electronic state.[10−13,41,42] The usefulness of our explanation is now recognized by many other researchers.[4,14,15,18]

Conclusions

Excited-state dependence of ESIPT of OHBAs in the vapor phase has been studied by means of emission spectroscopy. Substituent effects on the $S_1(\pi) \rightarrow S_0$ and $S_2(\pi) \rightarrow S_0$ fluorescence quantum yields can be explained in terms of our "nodal plane" model. The nodal plane model adds a simple, but rather powerful concept for the understanding of ESIPT. The utility of OHBA as a probe of the ESIPT mechanism is very useful for further studies.

Acknowledgment. S.N. expresses his sincere thanks to Professor Noboru Hirota of Kyoto University for his continuous encouragement. S.N. and U.N. are indebted to Dr. Hans Peter Luethi of Swiss Center for Scientific Computing for his polishing up our English in the paper and to Dr. Ken-ichi Sakai of Japan Advanced Institute of Science and Technology for his help in the setup of the CNDO/S3 program. The authors thank the Computer Center of the Institute for Molecular Science for the use of the IBM SP2, NEC SX-3/34R, and HSP computer and the Library Programs Gaussian 92 and QCPE #261. This work was partly supported by Grants-in-Aid for Scientific Research (B) Grant 03453012 and for Scientific Research on Priority Area "Quantum Tunneling of Group of Atoms as Systems with Many Degrees of Freedom" (Area 271/08240231) from The Ministry of Education, Science, Sports and Culture of Japan.

Supporting Information Available: Experimental details of 2-hydroxybenzoyl chloride, 2-(trichloroacetyl)phenol, 2-hydroxybenzoyl cyanide, and salicylamide. Absorption and fluorescence spectra of OHBAs, computational method and procedure, and optimized geometries of OHBAs (10 pages). Ordering information is given on any current masthead page.

References and Notes

(1) Klöpffer, W. *Adv. Photochem.* **1977**, *10*, 311.
(2) Rentzepis, P. M.; Barbara, P. F. *Adv. Chem. Phys.* **1981**, *47* (2), 627.
(3) Huppert, D.; Gutman, M.; Kaufmann, K. J. *Adv. Chem. Phys.* **1981**, *47* (2), 643.
(4) Barbara, P. F.; Walsh, P. K.; Brus, L. E. *J. Phys. Chem.* **1989**, *93*, 29 (Feature Article).
(5) *Spectroscopy and Dynamics of Elementary Proton Transfer in Polyatomic Systems*; Barbara, P. F., Trommsdorff, H. P., Hochstrasser, R. M., Hofacker, G. L., Eds.; *Chem. Phys.* **1989**, *136*, 153−360.
(6) *M. Kasha Festschrift*; Barbara, P. F., Nicol, M., El-Sayed, M. A., Eds.; *J. Phys. Chem.* **1991**, *95*, 10215−10524.
(7) *Proceedings of the 54th Okazaki Conference: Dynamic Studies on Hydrogen Atom Transfer Reactions*; Shizuka, H., Ed.; Institute for Molecular Science/Gunma University: Okazaki/Kiryu, 1996.
(8) Haddon, R. C.; Stillinger, F. H. In *Molecular Electronic Devices*; Carter, F. L., Ed.; Marcel Dekker: New York, 1982; Chapter II.
(9) Sixl, H.; Higelin, D. In *Molecular Electronic Devices II*; Carter, F. L., Ed.; Marcel Dekker: New York, 1987; Part I-2.
(10) Nagaoka, S.; Fujita, M.; Takemura, T.; Baba, H. *Chem. Phys. Lett.* **1986**, *123*, 489.
(11) Nagaoka, S.; Nagashima, U.; Ohta, N.; Fujita, M.; Takemura, T. *J. Phys. Chem.* **1988**, *92*, 166.
(12) Nagaoka, S.; Nagashima, U. *Chem. Phys.* **1989**, *136*, 153.
(13) Nagaoka, S. *Kagaku to Kogyo (Tokyo)* **1991**, *44*, 182.
(14) Grabowska, A.; Mordziński, A.; Tamai, N.; Yoshihara, K. *Chem. Phys. Lett.* **1988**, *153*, 389.
(15) Herek, J. L.; Pedersen, S.; Bañares, L.; Zewail, A. H. *J. Chem. Phys.* **1992**, *97*, 9046.
(16) Sobolewski, A. L.; Domcke, W. *Chem. Phys.* **1994**, *184*, 115.
(17) Vener, M. V.; Scheiner, S. *J. Phys. Chem.* **1995**, *99*, 642.
(18) Bisht, P. B.; Petek, H.; Yoshihara, K.; Nagashima, U. *J. Chem. Phys.* **1995**, *103*, 5290.

(19) Sobolewski, A. L.; Domcke, W. In *The Reaction Path in Chemistry: Current Approaches and Perspectives*; Heidrich, D., Ed.; Kluwer Academic: Amsterdam, 1995; pp 257−282.
(20) Douhal, A.; Lahmani, F.; Zewail, A. H. *Chem. Phys.* **1996**, *207*, 477.
(21) Mimuro, M.; Nagashima, U.; Nagaoka, S.; Nishimura, Y.; Takaichi, S.; Katoh, T.; Yamazaki, I. *Chem. Phys. Lett.* **1992**, *191*, 219.
(22) Mimuro, M.; Nishimura, Y.; Takaichi, S.; Yamano, Y.; Ito, M.; Nagaoka, S.; Yamazaki, I.; Katoh, T.; Nagashima, U. *Chem. Phys. Lett.* **1993**, *213*, 576.
(23) Benoiton, L.; Rydon, H. N.; Willett, J. E. *Chem. Ind. (London)* **1960**, 1060. Matsumoto, S.; Kobayashi, H.; Ueno, K. *Bull. Chem. Soc. Jpn.* **1969**, *42*, 960.
(24) Bosshard, H. H.; Mory, R.; Schmid, M.; Zollinger, Hch. *Helv. Chim. Acta* **1959**, *42*, 1653. Sen, A. B.; Sen Gupta, A. K. *J. Indian Chem. Soc.* **1956**, *33*, 437. Tiwari, S. S.; Tripathi, B. N. *J. Indian Chem. Soc.* **1956**, *33*, 214.
(25) Mimuro, M.; Murakami, A.; Fujita, Y. *Arch. Biochem. Biophys.* **1982**, *215*, 266.
(26) Melhuish, W. H. *J. Phys. Chem.* **1961**, *65*, 229.
(27) Inamoto, N. *Hammett Soku*; Maruzen: Tokyo, 1983. Johnson, C. D. *The Hammett Equation*; Cambridge University: London, 1973. Tsuno, Y.; Fujio, M. *Chem. Soc. Rev.* **1996**, 129.
(28) Smith, K. K.; Kaufmann, K. J. *J. Phys. Chem.* **1978**, *82*, 2286.
(29) Nagaoka, S.; Hirota, N.; Sumitani, M.; Yoshihara, K. *J. Am. Chem. Soc.* **1983**, *105*, 4220.
(30) Nagaoka, S.; Hirota, N.; Sumitani, M.; Yoshihara, K. Lipczynska-Kochany, E.; Iwamura, H. *J. Am. Chem. Soc.* **1984**, *106*, 6913.
(31) Mordziński, A.; Grellmann, K. H. *J. Phys. Chem.* **1986**, *90*, 5503.
(32) Englman, R.; Jortner, J. *Mol. Phys.* **1970**, *18*, 145.
(33) Catalán, J.; Toribio, F.; Acuña, A. U. *J. Phys. Chem.* **1982**, *86*, 303.
(34) Nagaoka, S.; Nagashima, U. *Chem. Phys.* **1996**, *206*, 353.
(35) Berlman, I. B. *Handbook of Fluorescence Spectra of Aromatic Molecules*, 2nd ed.; Academic Press: New York, 1971.
(36) Heimbrook, L. A.; Kenny, J. E.; Kohler, B. E.; Scott, G. W. *J. Chem. Phys.* **1981**, *75*, 5201.
(37) Felker, P. M.; Lambert, Wm. R.; Zewail, A. H. *J. Chem. Phys.* **1982**, *77*, 1603.
(38) Heimbrook, L. A.; Kenny, J. E.; Kohler, B. E.; Scott, G. W. *J. Phys. Chem.* **1983**, *87*, 280.
(39) Nishiya, T.; Yamauchi, S.; Hirota, N.; Baba, M.; Hanazaki, I. *J. Phys. Chem.* **1986**, *90*, 5730.
(40) Birks, J. B. *Photophysics of Aromatic Molecules*; Wiley-Interscience: London, 1970; p 88.
(41) Nagaoka, S.; Nagashima, U. *J. Phys. Chem.* **1990**, *94*, 1425.
(42) Nagaoka, S.; Nagashima, U. *J. Phys. Chem.* **1991**, *95*, 4006.